# Quantized Distributed Reception for MIMO Wireless Systems Using Spatial Multiplexing

Junil Choi, *Member, IEEE*, David J. Love, *Fellow, IEEE*, D. Richard Brown, III, *Senior Member, IEEE*, and Mireille Boutin

***Abstract*—We study a quantized distributed reception scenario in which a transmitter equipped with multiple antennas sends multiple streams via spatial multiplexing to a large number of geographically separated single antenna receive nodes. This approach is applicable to scenarios such as those enabled by the Internet of Things (IoT) which holds much commercial potential and could facilitate distributed multiple-input multiple-output (MIMO) communication in future systems. The receive nodes quantize their received signals and forward the quantized received signals to a receive fusion center. With global channel knowledge and forwarded quantized information from the receive nodes, the fusion center attempts to decode the transmitted symbols. We assume the transmit vector consists of arbitrary constellation points, and each receive node quantizes its received signal with one bit for each of the real and imaginary parts of the signal to minimize the transmission overhead between the receive nodes and the fusion center. Fusing this data is a nontrivial problem because the receive nodes cannot decode the transmitted symbols before quantization. We develop an optimal maximum likelihood (ML) receiver and a low-complexity zero-forcing (ZF)-type receiver at the fusion center. Despite its suboptimality, the ZF-type receiver is simple to implement and shows comparable performance with the ML receiver in the low signal-to-noise ratio (SNR) regime but experiences an error rate floor at high SNR. It is shown that this error floor can be overcome by increasing the number of receive nodes.**

***Index Terms*—Internet of things (IoT), multiple-input multiple-output (MIMO), quantized distributed reception, spatial multiplexing.**

## I. Introduction

As more and more internet-enabled things are commonly used (e.g., computers, smartphones, tablets, home appliances, sensors, and more), the Internet of Things (IoT) will change the paradigm of communication systems [1]. In the IoT environment, devices could be used as distributed transmit and/or receive entities allowing massive distributed multiple-input multiple-output (MIMO) systems to be implemented. Potentially, a large number of built-in sensors in the home, used to monitor the environment or actuate devices such as bulbs or locks, could be exploited as transmit/receive entities to support data transmission by smartphones or labtops. Among many possible scenarios, we focus on distributed reception for wireless communication systems in this paper.

Distributed reception for wireless communication systems is used to provide reliable communication between a transmitter and a receive fusion center via the help of geographically separated receive nodes [2]. Wireless channels between the transmitter and the multiple receive nodes are usually well modeled as independent, resulting in increased diversity gain, and the fusion center estimates the transmitted data using processed information from the receive nodes. Preliminary distributed reception techniques are now adopted in 3GPP LTE-Advanced in the context of coordinated multipoint (CoMP) reception scenario for cellular systems [3]–[6] and advanced information theoretic approaches for fronthaul/backhaul compression for cloud radio access networks have been proposed in [7]–[9].

There are strong similarities between distributed reception for wireless communication systems and wireless sensor networks (WSNs), where the former is aimed at data communications and the latter is more focused on environment classifications. WSNs have been extensively studied in references such as [10]–[21]. Many of the works on WSNs can be applied to distributed reception for wireless communication systems. Instead of reusing hand-optimized processing and fusion rules as in [19]–[21] for WSNs when performing distributed reception of a communication signal, it was shown in [22], [23] that by adopting appropriate channel codes we can obtain simple, yet powerful processing and decoding rules that have good symbol error rate (SER) performance for a practical range of signal-to-noise ratios (SNRs). Recently, [24] showed that even simple combining of hard decisions at the receive nodes can give performance within 2 dB SNR of ideal receive beamforming for wireless communication systems.

However, most of the prior work on WSNs and distributed reception for wireless communication systems considered only detection/estimation of a single-dimensional parameter or single transmitted symbol. To our knowledge, there are few papers that discuss multi-dimensional estimation problems. A few exceptions can be found in [25], [26] which consider the estimation of a multi-dimensional vector in WSNs with additive noise at each sensor.

Manuscript received September 26, 2014; revised January 26, 2015; accepted April 01, 2015. Date of publication April 17, 2015; date of current version June 04, 2015. The associate editor coordinating the review of this manuscript and approving it for publication was Dr. Joakim Jalden.

J. Choi is with the Department of Electrical and Computer Engineering, The University of Texas at Austin, Austin, TX 78712 USA (e-mail: junil.choi@utexas.edu).

D. J. Love and M. Boutin are with the School of Electrical and Computer Engineering, Purdue University, West Lafayette, IN 47907 USA (e-mail: djlove@purdue.edu; mboutin@purdue.edu).

D. R. Brown, III, is with the Department of Electrical and Computer Engineering, Worcester Polytechnic Institute, Worcester, MA 01609 USA (e-mail: drb@wpi.edu).

Color versions of one or more of the figures in this paper are available online at http://ieeexplore.ieee.org.

Digital Object Identifier 10.1109/TSP.2015.2424193

In this paper, we consider distributed MIMO communication systems where the transmitter is equipped with multiple antennas and simultaneously transmits independent data symbols using spatial multiplexing to a set of geographically separated receive nodes deployed with a single receive antenna sent through independent fading channels. Each receive node quantizes its received signal and forwards the quantized signal to the fusion center. The fusion center then attempts to decode the transmitted data by exploiting the quantized signals from the receive nodes and global channel information. This scenario, i.e., quantized distributed reception, is likely to become popular with the emergence of massive MIMO systems [27] and IoT because base stations tend to be equipped with a large number of antennas in massive MIMO systems and we can easily have a large number of receive nodes in an IoT environment.

For practical purposes, we assume each receive node quantizes its received signal with one bit per real part and one bit per imaginary part of the received signal to minimize the transmission overhead between the receive nodes and the fusion center. Quantizer design is a non-trivial problem because the receive nodes are not able to decode the transmitted symbols due to the fact that each receive node has only one antenna [28]. Instead, each receive node quantizes a single quantity, i.e., the received signal, regardless of the number of transmitted symbols. In this setup, we develop an optimal maximum likelihood (ML) receiver and a low-complexity zero-forcing (ZF)-type receiver[1] assuming global channel knowledge at the fusion center. The ML receiver outperforms the ZF-type receiver regardless of the number of receive nodes and SNR ranges. However, the complexity of the ML receiver is excessive, especially when the number of transmitted symbols becomes large. On the other hand, the ZF-type receiver can be easily implemented and gives comparable performance to that of the ML receiver when the SNR is low to moderate, although it suffers from an error rate floor when SNR is high. The error rate floor of the ZF-type receiver can be easily mitigated by having more receive nodes.

When the SNR is high, the quantized distributed reception problem is closely tied to work in quantized frame expansion. Linear transformation and expansion by a frame matrix in the presence of coefficient quantization is thoroughly studied in [31], [32]. A linear expansion method, which is similar to our ZF-type receiver, and its performance in terms of the mean-squared error (MSE) were analyzed based on the properties of a frame matrix, and an advanced non-linear expansion method relying on linear programming was also studied. The major difference compared to our problem setting is that [31], [32] do not assume any additive noise before quantization, while our scenario considers a fading channel (which corresponds to a frame matrix in frame expansion) with additive noise prior to quantization at the receive nodes. We rely on some of the analytical results from [31] for evaluating and modifying our ZF-type receiver later.

The rest of the paper is organized as follows. In Section II, we define our system model. The ML and ZF-type receivers are proposed and their characteristics are compared in Section III. Simulation results that evaluate the proposed receivers are shown in Section IV, and conclusions follow in Section V.

*Notation:* Lower and upper boldface symbols denote column vectors and matrices, respectively. $\|\mathbf{x}\|$ represents the two-norm of a vector $\mathbf{x}$, and $(\cdot)^T, (\cdot)^H, (\cdot)^\dagger$ are used to denote transpose, Hermitian transpose, and pseudo inverse of their argument, respectively. $\mathrm{Re}(c)$ and $\mathrm{Im}(c)$ denote the real and complex part of a complex number $c$, respectively. $\mathbf{0}_m$ represents an $m \times 1$ all zero vector, $\mathbf{1}_m$ denotes an $m \times 1$ all one vector, and $\mathbf{I}_m$ is used for $m \times m$ identity matrix. The expectation operation is denoted by $\mathrm{E}[\cdot]$, and $\Pr(A)$ denotes the probability of event $A$.

## II. System Model

We consider a network consisting of a transmitter with $N_t$ antennas, communicating with a receive fusion center that is connected to $K$ geographically separated, single antenna receive nodes. The transmitter tries to send $N_t$ independent data symbols simultaneously by spatial multiplexing[2] to the fusion center via the help of the receive nodes. The received signal at the $k$-th receive node is given as

$$y_k = \sqrt{\frac{\rho}{N_t}}\mathbf{h}_k^H \mathbf{x} + n_k, \quad k = 1, \ldots, K \tag{1}$$

where $\rho$ is the transmit SNR, $\mathbf{h}_k \in \mathbb{C}^{N_t}$ is the independent and identically distributed (i.i.d.) Rayleigh fading channel vector between the transmitter and the $k$-th receive node, $n_k$ is complex additive white Gaussian noise (AWGN) distributed as $\mathcal{CN}(0,1)$ at the $k$-th node, and $\mathbf{x} = [x_1, \ldots, x_{N_t}]^T$ is the transmitted signal vector. We assume $x_i \in \mathcal{S}$ is from a standard $M$-ary constellation

$$\mathcal{S} = \{s_1, \ldots, s_M\} \subset \mathbb{C}$$

which satisfies $\mathrm{E}[\|\mathbf{x}\|^2] = N_t$ and $\mathrm{E}[\mathbf{x}] = \mathbf{0}_{N_t}$. The input-output relation in (1) can be also written as

$$\mathbf{y} = \sqrt{\frac{\rho}{N_t}}\mathbf{H}\mathbf{x} + \mathbf{n}$$

where

$$\mathbf{y} = [\, y_1 \quad y_2 \quad \cdots \quad y_K \,]^T,$$
$$\mathbf{n} = [\, n_1 \quad n_2 \quad \cdots \quad n_K \,]^T,$$
$$\mathbf{H} = [\, \mathbf{h}_1 \quad \mathbf{h}_2 \quad \cdots \quad \mathbf{h}_K \,]^H.$$

We further assume that the fusion center can access the full knowledge[3] of $\mathbf{h}_k$ for all $k$.

If the fusion center has full knowledge of $y_k$ for all $k$, then the optimal receiver is given as

$$\hat{\mathbf{x}}_{\mathrm{opt}} = \underset{\mathbf{x}' \in \mathcal{S}^{N_t}}{\mathrm{argmin}} \left\| \mathbf{y} - \sqrt{\frac{\rho}{N_t}}\mathbf{H}\mathbf{x}' \right\|^2$$

where $\mathcal{S}^n$ is the cartesian product of $\mathcal{S}$ of order $n$. However, we are interested in the scenario when each receive node *quantizes* its received signal and conveys the quantized received signal,

[1]The proposed receivers in this paper also can be applied to massive MIMO detection problems [29], [30].

[2]The transmitter also can send a number of symbols smaller than $N_t$ by adopting precoding or antenna selection, which is outside the scope of this paper.

[3]Recently, we developed channel estimation techniques for the scenario of this paper in [33].

$\hat{y}_k$, to the fusion center. Therefore, the fusion center needs to use other approaches to decode the transmitted symbols in our problem.

We assume $\hat{y}_k$ can be forwarded from the $k$-th receive node to the fusion center without any error. This assumption would be reasonable because the receive nodes and the fusion center are usually connected by a very high-rate link or located near each other in practice. We further assume that the forward link transmission and the LAN are operated on different time or frequency resources to prevent interference between the two.

To make the problem practical, we assume that the receive nodes only can perform very simple operation, i.e., they do not decode the transmitted vector $\mathbf{x}$ but instead simply quantize $y_k$ directly. Moreover, to minimize the data transmission overhead from the receive nodes to the fusion center, we assume each receive node quantizes $y_k$ using two bits, i.e., one bit for each of the real and imaginary parts of $y_k$. Thus, the quantized received signal $\hat{y}_k$ can be written as

$$\hat{y}_k = \mathrm{sgn}(\mathrm{Re}(y_k) - \tau_{\mathrm{Re},k}) + j(\mathrm{sgn}(\mathrm{Im}(y_k) - \tau_{\mathrm{Im},k}))$$

where $\mathrm{sgn}(\cdot)$ is the sign function defined as

$$\mathrm{sgn}(x) = \begin{cases} 1 & \text{if } x \geq 0 \\ -1 & \text{if } x < 0 \end{cases},$$

and $\tau_{\mathrm{Re},k}$ and $\tau_{\mathrm{Im},k}$ are quantization thresholds of the real and imaginary parts of $y_k$ at user $k$, respectively.

With a given realization of $\mathbf{h}_k$, we consider the simple, yet effective, thresholds

$$\tau_{\mathrm{Re},k} = \mathrm{E}[\mathrm{Re}(y_k)] = \mathrm{E}\left[\sqrt{\frac{\rho}{N_t}}\mathrm{Re}(\mathbf{h}_k^H\mathbf{x}) + \mathrm{Re}(n_k)\right] = 0,$$
$$\tau_{\mathrm{Im},k} = \mathrm{E}[\mathrm{Im}(y_k)] = \mathrm{E}\left[\sqrt{\frac{\rho}{N_t}}\mathrm{Im}(\mathbf{h}_k^H\mathbf{x}) + \mathrm{Im}(n_k)\right] = 0,$$

where equalities are based on the assumption that $n_k$ is distributed as $\mathcal{CN}(0,1)$, or equivalently $\mathrm{Re}(n_k)$ and $\mathrm{Im}(n_k)$ are independent and both distributed as $\mathcal{N}(0,\frac{1}{2})$, and the entries of $\mathbf{x}$ are independently drawn from $\mathcal{S}^{N_t}$ with equal probabilities, which gives $\mathrm{E}[\mathrm{Re}(\mathbf{c}^T\mathbf{x})] = 0$ and $\mathrm{E}[\mathrm{Im}(\mathbf{c}^T\mathbf{x})] = 0$ for an arbitrary combining vector $\mathbf{c} \in \mathbb{C}^{N_t}$. Although simple, these thresholds are consistent with the optimal threshold design studied in [25] in an average sense. We assume the quantization thresholds $\tau_{\mathrm{Re},k} = 0$ and $\tau_{\mathrm{Im},k} = 0$ for the remainder of this paper.

Once the fusion center receives $\hat{y}_k$ from all receive nodes, it attempts to decoded the transmitted data symbols $\mathbf{x}$ using the forwarded information and channel knowledge. We define

$$\hat{\mathbf{y}} = [\,\hat{y}_1 \quad \hat{y}_2 \quad \cdots \quad \hat{y}_K\,]^T$$

which is useful in Section III.B. The conceptual explanation of the scenario is depicted in Fig. 1.

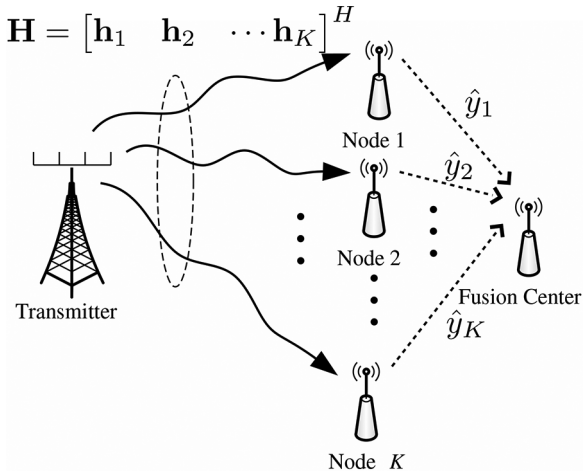


Fig. 1. The conceptual figure of distributed reception with multiple antennas at the transmitter. Each receive node is equipped with a single receive antenna.

## III. Quantized Distributed Reception Techniques

With the knowledge of $\mathbf{H}$ and $\hat{\mathbf{y}}$ at the fusion center, we can implement different kinds of receivers considering complexity and performance. We first develop an optimal ML receiver and low-complexity ZF-type receiver. Then, we discuss the performance of receivers regarding system parameters such as $\rho$ and $K$. We also explain a possible modification of the ZF-type receiver and analyze the achievable rate of quantized distributed reception.

### A. ML Receiver

We convert the problem of interest to the real domain to facilitate analysis. This can be done by defining $\mathbf{H}_{\mathrm{R},k} \in \mathbb{R}^{2\times 2N_t}$, $\mathbf{x}_{\mathrm{R}} \in \mathbb{R}^{2N_t}$ and $\mathbf{n}_{\mathrm{R},k} \in \mathbb{R}^2$ as

$$\mathbf{H}_{\mathrm{R},k} = \begin{bmatrix} \mathrm{Re}\left(\mathbf{h}_k^T\right) & \mathrm{Im}\left(\mathbf{h}_k^T\right) \\ -\mathrm{Im}\left(\mathbf{h}_k^T\right) & \mathrm{Re}\left(\mathbf{h}_k^T\right) \end{bmatrix} = \begin{bmatrix} \mathbf{h}_{\mathrm{R},k,1}^T \\ \mathbf{h}_{\mathrm{R},k,2}^T \end{bmatrix},$$
$$\mathbf{x}_{\mathrm{R}} = \begin{bmatrix} \mathrm{Re}(\mathbf{x}) \\ \mathrm{Im}(\mathbf{x}) \end{bmatrix}, \quad \mathbf{n}_{\mathrm{R},k} = \begin{bmatrix} \mathrm{Re}(n_k) \\ \mathrm{Im}(n_k) \end{bmatrix}$$

where

$$\mathbf{h}_{\mathrm{R},k,1} = \begin{bmatrix} \mathrm{Re}(\mathbf{h}_k) \\ \mathrm{Im}(\mathbf{h}_k) \end{bmatrix}, \quad \mathbf{h}_{\mathrm{R},k,2} = \begin{bmatrix} -\mathrm{Im}(\mathbf{h}_k) \\ \mathrm{Re}(\mathbf{h}_k) \end{bmatrix}.$$

Then, the received signal $y_k$ also can be rewritten in the real domain as

$$\mathbf{y}_{\mathrm{R},k} = \begin{bmatrix} y_{\mathrm{R},k,1} \\ y_{\mathrm{R},k,2} \end{bmatrix} = \begin{bmatrix} \mathrm{Re}(y_k) \\ \mathrm{Im}(y_k) \end{bmatrix} = \sqrt{\frac{\rho}{N_t}}\mathbf{H}_{\mathrm{R},k}\mathbf{x}_{\mathrm{R}} + \mathbf{n}_{\mathrm{R},k},$$

and the vectorized version of the quantized $\hat{y}_k$ in the real domain is given as

$$\hat{\mathbf{y}}_{\mathrm{R},k} = \begin{bmatrix} \hat{y}_{\mathrm{R},k,1} \\ \hat{y}_{\mathrm{R},k,2} \end{bmatrix} = \begin{bmatrix} \mathrm{sgn}(\mathrm{Re}(y_k)) \\ \mathrm{sgn}(\mathrm{Im}(y_k)) \end{bmatrix}. \tag{2}$$

Once the fusion center receives $\hat{\mathbf{y}}_{\mathrm{R},k}$ from all receive nodes, it generates the *sign-refined* channel matrix $\widetilde{\mathbf{H}}_{\mathrm{R},k}$ according to

$$\widetilde{\mathbf{H}}_{\mathrm{R},k} = \begin{bmatrix} \widetilde{\mathbf{h}}_{\mathrm{R},k,1}^T \\ \widetilde{\mathbf{h}}_{\mathrm{R},k,2}^T \end{bmatrix}$$

where $\widetilde{\mathbf{h}}_{\mathrm{R},k,i}$ is defined as

$$\widetilde{\mathbf{h}}_{\mathrm{R},k,i} = \hat{y}_{\mathrm{R},k,i}\mathbf{h}_{\mathrm{R},k,i}. \tag{3}$$

Because $\hat{y}_{\mathrm{R},k,i}$ is $\pm 1$, (3) can be considered as a sign refinement of $\mathbf{h}_{\mathrm{R},k,i}$. We let $\mathcal{S}_{\mathrm{R}}$ be

$$\mathcal{S}_{\mathrm{R}} = \left\{ \begin{bmatrix} \mathrm{Re}(s_1) \\ \mathrm{Im}(s_1) \end{bmatrix}, \ldots, \begin{bmatrix} \mathrm{Re}(s_M) \\ \mathrm{Im}(s_M) \end{bmatrix} \right\}$$

where $M$ is the size of the constellation $\mathcal{S}$. We also define two sets $\mathcal{P}$ and $\mathcal{N}$ using $\{y_{\mathrm{R},k,i}\}$ for $k \in \{1,\ldots,K\}$ and $i \in \{1,2\}$ as

$$\mathcal{P} = \{(k,i) : y_{\mathrm{R},k,i} \geq 0\}, \quad \mathcal{N} = \{(k,i) : y_{\mathrm{R},k,i} < 0\}.$$

With these definitions, we can define a likelihood function as

$$\begin{aligned} L(\mathbf{x}'_{\mathrm{R}}) &= \Pr\left( \sqrt{\frac{\rho}{N_t}} \mathbf{h}_{\mathrm{R},k,i}^T \mathbf{x}'_{\mathrm{R}} + n_{\mathrm{R},k,i} \geq 0 \middle| \forall (k,i) \in \mathcal{P} \right) \\ &\quad \cdot \Pr\left( \sqrt{\frac{\rho}{N_t}} \mathbf{h}_{\mathrm{R},k,i}^T \mathbf{x}'_{\mathrm{R}} + n_{\mathrm{R},k,i} < 0 \middle| \forall (k,i) \in \mathcal{N} \right) \\ &\overset{(a)}{=} \Pr\left( \sqrt{\frac{\rho}{N_t}} \widetilde{\mathbf{h}}_{\mathrm{R},k,i}^T \mathbf{x}'_{\mathrm{R}} \geq -n_{\mathrm{R},k,i} \middle| \forall (k,i) \in \mathcal{P} \right) \\ &\quad \cdot \Pr\left( \sqrt{\frac{\rho}{N_t}} \widetilde{\mathbf{h}}_{\mathrm{R},k,i}^T \mathbf{x}'_{\mathrm{R}} \geq n_{\mathrm{R},k,i} \middle| \forall (k,i) \in \mathcal{N} \right) \\ &\overset{(b)}{=} \Pr\left( \sqrt{\frac{\rho}{N_t}} \widetilde{\mathbf{h}}_{\mathrm{R},k,i}^T \mathbf{x}'_{\mathrm{R}} \geq -n_{\mathrm{R},k,i} \middle| \forall (k,i) \in \mathcal{P} \right) \\ &\quad \cdot \Pr\left( \sqrt{\frac{\rho}{N_t}} \widetilde{\mathbf{h}}_{\mathrm{R},k,i}^T \mathbf{x}'_{\mathrm{R}} \geq -n_{\mathrm{R},k,i} \middle| \forall (k,i) \in \mathcal{N} \right) \\ &\overset{(c)}{=} \prod_{i=1}^{2} \prod_{k=1}^{K} \Phi\left( \sqrt{\frac{2\rho}{N_t}} \widetilde{\mathbf{h}}_{\mathrm{R},k,i}^T \mathbf{x}'_{\mathrm{R}} \right) \end{aligned}$$

where $\Phi(t) = \int_{-\infty}^{t} \frac{1}{\sqrt{2\pi}} e^{-\frac{\tau^2}{2}} d\tau$, $(a)$ is based on the sign refinement in (3), $(b)$ is because $n_{\mathrm{R},k,i}$ and $-n_{\mathrm{R},k,i}$ have the same distribution (or the same probability density function) such that $\Pr(c \geq n_{\mathrm{R},k,i}) = \Pr(c \geq -n_{\mathrm{R},k,i})$ for an arbitrary constant $c$, and $(c)$ comes from the fact that $n_{\mathrm{R},k,i}$ is independent for all $k$ and $i$ and from distribution $\mathcal{N}(0, \frac{1}{2})$. Then, the ML receiver is given as[4]

$$\hat{\mathbf{x}}_{\mathrm{R,ML}} = \underset{\mathbf{x}'_{\mathrm{R}} \in \mathcal{S}_{\mathrm{R}}^{N_t}}{\mathrm{argmax}} \prod_{i=1}^{2} \prod_{k=1}^{K} \Phi\left( \sqrt{\frac{2\rho}{N_t}} \widetilde{\mathbf{h}}_{\mathrm{R},k,i}^T \mathbf{x}'_{\mathrm{R}} \right). \tag{4}$$

The complexity of the exhaustive search of the ML receiver increases exponentially with the number of transmit symbols in spatial multiplexing, i.e., we need to search over $M^{N_t}$ elements. Therefore, in practice, it is desired to implement a low complexity receiver for large numbers of transmit antennas.

*Remark 1:* If the number of receive nodes $K$ is less than the number of transmit antennas $N_t$, then the decoding performance at the fusion center would be very poor. This situation will likely not hold for our problem setting because we can easily have $K \gg N_t$ based on the IoT environment.

*Remark 2:* Instead of quantizing both the real and imaginary parts of the received signal at each node, we can have the same performance on average by quantizing and forwarding only the real *or* imaginary part of the received signal with twice the number of receive nodes. This is based on the assumption that the real and imaginary parts of the noise $n_k$ are i.i.d. for all $k$.

[4]A similar ML receiver is also derived in [25].

### B. Low-Complexity Zero-Forcing-Type Receiver

The ML receiver defined in (4) has no constraint on the norm of the transmit vector $\mathbf{x}$. To develop our ZF-type receiver, however, we assume $\|\mathbf{x}\|^2 = N_t$. If $\mathcal{S}$ is a phase shift keying (PSK) constellation with $|s_m|^2 = 1$ for all $m$, this constraint is trivially satisfied. Even for a quadrature amplitude modulation (QAM) constellation (that is properly normalized), the constraint can be approximately satisfied because

$$\sum_{i=1}^{N_t} |x_i|^2 \approx N_t$$

when $N_t$ is large and $x_i$ is drawn from $\mathcal{S}$ with equal probabilities. Simulation results in Section IV show that our ZF-type receiver works even with not-so-large $N_t$, e.g., $N_t = 10$.

Before proposing our ZF-type receiver, we first state the following lemma which establishes the theoretical foundation of our receiver.

*Lemma 1:* Define a matrix $\widetilde{\mathbf{H}}_{\mathrm{R,S}} \in \mathbb{R}^{2K \times 2N_t}$ by stacking $\widetilde{\mathbf{H}}_{\mathrm{R},k}$ as

$$\widetilde{\mathbf{H}}_{\mathrm{R,S}} = \begin{bmatrix} \widetilde{\mathbf{H}}_{\mathrm{R},1}^T & \widetilde{\mathbf{H}}_{\mathrm{R},2}^T & \cdots & \widetilde{\mathbf{H}}_{\mathrm{R},K}^T \end{bmatrix}^T, \tag{5}$$

and let $\mathbf{t}(\mathbf{x}'_{\mathrm{R}})$ be

$$\begin{aligned} \mathbf{t}(\mathbf{x}'_{\mathrm{R}}) &= \begin{bmatrix} t_1(\mathbf{x}'_{\mathrm{R}}) & t_2(\mathbf{x}'_{\mathrm{R}}) & \cdots & t_{2K}(\mathbf{x}'_{\mathrm{R}}) \end{bmatrix}^T, \\ t_\ell(\mathbf{x}'_{\mathrm{R}}) &= \widetilde{\mathbf{h}}_{\mathrm{R},k,i}^T \mathbf{x}'_{\mathrm{R}} \end{aligned}$$

where $\ell = 2(k-1) + i$ for $k = 1,\ldots,K$ and $i = 1,2$. Note that $\|\mathbf{x}'_{\mathrm{R}}\|^2 = N_t$ based on the assumption. Then the likelihood function $L(\mathbf{x}'_{\mathrm{R}})$ is upper bounded as

$$\begin{aligned} L(\mathbf{x}'_{\mathrm{R}}) &= \prod_{i=1}^{2} \prod_{k=1}^{K} \Phi\left( \sqrt{\frac{2\rho}{N_t}} \widetilde{\mathbf{h}}_{\mathrm{R},k,i}^T \mathbf{x}'_{\mathrm{R}} \right) \\ &= \prod_{\ell=1}^{2K} \Phi\left( \sqrt{\frac{2\rho}{N_t}} t_\ell(\mathbf{x}'_{\mathrm{R}}) \right) \\ &\leq \prod_{\ell=1}^{2K} \Phi\left( \sqrt{\frac{\rho}{K}} \|\widetilde{\mathbf{H}}_{\mathrm{R,S}}\|_{\mathrm{A}} \right) \end{aligned}$$

when $t_\ell(\mathbf{x}'_{\mathrm{R}}) = \sqrt{\frac{N_t}{2K}} \|\widetilde{\mathbf{H}}_{\mathrm{R,S}}\|_{\mathrm{A}}$ for all $\ell$ where $\|\cdot\|_{\mathrm{A}}$ is an arbitrary matrix norm that is consistent with the vector two-norm.

*Proof:* To prove Lemma 1, we derive an upper bound of the maximum of $L(\mathbf{x}'_{\mathrm{R}})$ with the relaxed constraint $\mathbf{x}'_{\mathrm{R}} \in \mathbb{R}^{2N_t}$ instead of $\mathbf{x}'_{\mathrm{R}} \in \mathcal{S}_{\mathrm{R}}^{N_t}$. Note that the norm constraint $\|\mathbf{x}'_{\mathrm{R}}\|^2 = N_t$ still holds. With the definitions of $t_\ell(\mathbf{x}'_{\mathrm{R}})$ and $\mathbf{t}(\mathbf{x}'_{\mathrm{R}})$, we have

$$\begin{aligned} &\max_{\substack{\mathbf{x}'_{\mathrm{R}} \in \mathbb{R}^{2N_t}, \\ \|\mathbf{x}'_{\mathrm{R}}\|^2 = N_t}} L(\mathbf{x}'_{\mathrm{R}}) \\ &\quad = \max_{\substack{\mathbf{x}'_{\mathrm{R}} \in \mathbb{R}^{2N_t}, \\ \|\mathbf{x}'_{\mathrm{R}}\|^2 = N_t}} \prod_{i=1}^{2} \prod_{k=1}^{K} \Phi\left( \sqrt{\frac{2\rho}{N_t}} \widetilde{\mathbf{h}}_{\mathrm{R},k,i}^T \mathbf{x}'_{\mathrm{R}} \right) \\ &\quad \leq \max_{\substack{\mathbf{t}(\mathbf{x}'_{\mathrm{R}}) \in \mathbb{R}^{2K}, \\ \|\mathbf{t}(\mathbf{x}'_{\mathrm{R}})\|^2 \leq N_t \|\widetilde{\mathbf{H}}_{\mathrm{R,S}}\|_{\mathrm{A}}^2}} \prod_{\ell=1}^{2K} \Phi\left( \sqrt{\frac{2\rho}{N_t}} t_\ell(\mathbf{x}'_{\mathrm{R}}) \right) \end{aligned} \tag{6}$$

$$= \max_{\substack{\mathbf{t}(\mathbf{x}'_{\mathrm{R}})\in\mathbb{R}^{2K},\\ \|\mathbf{t}(\mathbf{x}'_{\mathrm{R}})\|^2\le N_t\|\widetilde{\mathbf{H}}_{\mathrm{R,S}}\|_{\mathrm{A}}^2,\\ t_\ell(\mathbf{x}'_{\mathrm{R}})>0,\forall\ell}} \prod_{\ell=1}^{2K}\Phi\left(\sqrt{\frac{2\rho}{N_t}}t_\ell(\mathbf{x}'_{\mathrm{R}})\right) \tag{7}$$

$$= \max_{\substack{\mathbf{t}(\mathbf{x}'_{\mathrm{R}})\in\mathbb{R}^{2K},\\ \|\mathbf{t}(\mathbf{x}'_{\mathrm{R}})\|^2= N_t\|\widetilde{\mathbf{H}}_{\mathrm{R,S}}\|_{\mathrm{A}}^2,\\ t_\ell(\mathbf{x}'_{\mathrm{R}})>0,\forall\ell}} \prod_{\ell=1}^{2K}\Phi\left(\sqrt{\frac{2\rho}{N_t}}t_\ell(\mathbf{x}'_{\mathrm{R}})\right) \tag{8}$$

where (6) is based on the fact that

$$\|\widetilde{\mathbf{H}}_{\mathrm{R,S}}\mathbf{x}'_{\mathrm{R}}\|^2 \le \|\widetilde{\mathbf{H}}_{\mathrm{R,S}}\|_{\mathrm{A}}^2\|\mathbf{x}'_{\mathrm{R}}\|^2 = N_t\|\widetilde{\mathbf{H}}_{\mathrm{R,S}}\|_{\mathrm{A}}^2,$$

and (7) is because $\Phi(a) > \Phi(0)$ for $a > 0$. Note that the inequality constraint on $\|\mathbf{t}(\mathbf{x}'_{\mathrm{R}})\|^2$ in (7) is changed to the equality constraint in (8).

The objective function in (8) is trivially bounded by one; however, there is a certain maximum point in our problem because of the norm constraint of $\|\mathbf{t}(\mathbf{x}'_{\mathrm{R}})\|^2 = N_t\|\widetilde{\mathbf{H}}_{\mathrm{R,S}}\|_{\mathrm{A}}^2$. Let $g_\ell = \sqrt{\frac{2\rho}{N_t}}t_\ell(\mathbf{x}'_{\mathrm{R}})$ and $\mathbf{g} = [\,g_1 \quad g_2 \quad \cdots \quad g_{2K}\,]^T$. Instead of finding the solution for (8) directly, we first find a local extrema of

$$\log\left[\prod_{\ell=1}^{2K}\Phi\left(\sqrt{\frac{2\rho}{N_t}}t_\ell(\mathbf{x}'_{\mathrm{R}})\right)\right] = \sum_{\ell=1}^{2K}\log\left[\Phi\left(\sqrt{\frac{2\rho}{N_t}}t_\ell(\mathbf{x}'_{\mathrm{R}})\right)\right] = \sum_{\ell=1}^{2K}\log\Phi(g_\ell) \tag{9}$$

by looking at the point at which the tangential derivatives to the circle $\|\mathbf{g}\|^2 = 2\rho\|\widetilde{\mathbf{H}}_{\mathrm{R,S}}\|_{\mathrm{A}}^2$ are equal to zero.[5] The tangential derivatives of (9) are given by

$$\left(g_n\frac{\partial}{\partial g_m} - g_m\frac{\partial}{\partial g_n}\right)\sum_{\ell=1}^{2K}\log\Phi(g_\ell) = g_n\frac{\Phi'(g_m)}{\Phi(g_m)} - g_m\frac{\Phi'(g_n)}{\Phi(g_n)}$$

for $n, m = 1, 2, \ldots, 2K$ and $n \neq m$. Setting the tangential derivatives equal to zero, we obtain the equations

$$g_n\frac{\Phi'(g_m)}{\Phi(g_m)} = g_m\frac{\Phi'(g_n)}{\Phi(g_n)}$$

or equivalently,

$$\frac{1}{g_m}\frac{\Phi'(g_m)}{\Phi(g_m)} = \frac{1}{g_n}\frac{\Phi'(g_n)}{\Phi(g_n)} \tag{10}$$

for $n, m = 1, 2, \ldots, 2K$ and $n \neq m$ because $g_\ell > 0$ for all $\ell$. Clearly, this system of equations is satisfied when $g_n = g_m$ for all $n, m = 1, 2, \ldots, 2K$. Under the constraint $\|\mathbf{g}\|^2 = 2\rho\|\widetilde{\mathbf{H}}_{\mathrm{R,S}}\|_{\mathrm{A}}^2$, one possible solution point is given as

$$g_\ell = \sqrt{\frac{\rho}{K}}\|\widetilde{\mathbf{H}}_{\mathrm{R,S}}\|_{\mathrm{A}} \tag{11}$$

[5]Because our searching space is restricted to the circle $\|\mathbf{g}\|^2 = 2\rho\|\widetilde{\mathbf{H}}_{\mathrm{R,S}}\|_{\mathrm{A}}^2$, the point where the tangential derivatives equal to zero is a local extrema of the objective function.

for all $\ell$. Note that the point in (11) is the only solution for (10) because

$$G(s) = \frac{1}{s}\Phi'(s)\frac{1}{\Phi(s)}$$

is a product of three functions that are strictly monotonically decreasing with $s \in (0, \infty)$, and thus $G(s)$ is also strictly monotonically decreasing with $s$.

Because $t_\ell(\mathbf{x}'_{\mathrm{R}}) = \sqrt{\frac{N_t}{2\rho}}g_\ell$, the point

$$t_\ell(\mathbf{x}'_{\mathrm{R}}) = \sqrt{\frac{N_t}{2K}}\|\widetilde{\mathbf{H}}_{\mathrm{R,S}}\|_{\mathrm{A}}$$

for $\ell = 1, \ldots, 2$ K is the only extreme point of the objective function in (8). We can show that the extreme point is indeed the maximum point of (8) by using the lemma in Appendix A. ■

Lemma 1 states that when $\mathbf{t}(\mathbf{x}'_{\mathrm{R}}) = \sqrt{\frac{N_t}{2K}}\|\widetilde{\mathbf{H}}_{\mathrm{R,S}}\|_{\mathrm{A}}\mathbf{1}_{2K}$, it maximizes the likelihood function with the norm constraint $\|\mathbf{t}(\mathbf{x}'_{\mathrm{R}})\|^2 = N_t\|\widetilde{\mathbf{H}}_{\mathrm{R,S}}\|_{\mathrm{A}}^2$. From the fact that

$$\mathbf{t}(\mathbf{x}'_{\mathrm{R}}) = \widetilde{\mathbf{H}}_{\mathrm{R,S}}\mathbf{x}'_{\mathrm{R}},$$

the vector $\check{\mathbf{x}}_{\mathrm{R}}$, which is given as

$$\check{\mathbf{x}}_{\mathrm{R}} = \widetilde{\mathbf{H}}_{\mathrm{R,S}}^{\dagger}\mathbf{t}(\mathbf{x}'_{\mathrm{R}}) = \sqrt{\frac{N_t}{2K}}\|\widetilde{\mathbf{H}}_{\mathrm{R,S}}\|_{\mathrm{A}}\widetilde{\mathbf{H}}_{\mathrm{R,S}}^{\dagger}\mathbf{1}_{2K},$$

would be a reasonable estimate for the transmitted vector.

To implement this receiver in terms of the quantized received signals, let $\hat{\mathbf{y}}_{\mathrm{R}}$ be

$$\hat{\mathbf{y}}_{\mathrm{R}} = [\,\hat{\mathbf{y}}_{\mathrm{R},1}^T \quad \hat{\mathbf{y}}_{\mathrm{R},2}^T \quad \cdots \quad \hat{\mathbf{y}}_{\mathrm{R},K}^T\,]^T$$

where $\hat{\mathbf{y}}_{\mathrm{R},k}$ is defined in (2). It is easy to show by using the relation between $\mathbf{H}_{\mathrm{R,S}}$ and $\widetilde{\mathbf{H}}_{\mathrm{R,S}}$ (or between their rows given in (3)) that

$$\widetilde{\mathbf{H}}_{\mathrm{R,S}}^{\dagger}\mathbf{1}_{2K} = \mathbf{H}_{\mathrm{R,S}}^{\dagger}\hat{\mathbf{y}}_{\mathrm{R}}$$

because the $i$-th row of $\widetilde{\mathbf{H}}_{\mathrm{R,S}}$ is the same as that of $\mathbf{H}_{\mathrm{R,S}}$ with the sign adjustment by the sign of the $i$-th element of $\hat{\mathbf{y}}_{\mathrm{R}}$. Based on these observations, we propose a ZF-type receiver at the fusion center, i.e., the fusion center generates $\check{\mathbf{x}}_{\mathrm{R,ZF}} \in \mathbb{R}^{2N_t}$ as

$$\check{\mathbf{x}}_{\mathrm{R,ZF}} = \mathbf{H}_{\mathrm{R,S}}^{\dagger}\hat{\mathbf{y}}_{\mathrm{R}}. \tag{12}$$

With $\mathbf{H}$ and $\hat{\mathbf{y}}$ which are defined in Section II, the same receiver with (12) can be implemented in the complex domain as

$$\check{\mathbf{x}}_{\mathrm{ZF}} = \mathbf{H}^{\dagger}\hat{\mathbf{y}} \tag{13}$$

where $\check{\mathbf{x}}_{\mathrm{ZF}} \in \mathbb{C}^{N_t}$.

Note that the squared norm of $\check{\mathbf{x}}_{\mathrm{ZF}}$ may not be $N_t$ anymore; however, the normalization term does not have any impact on PSK symbol decisions. If $x_i$ is from a QAM constellation, the normalization term is important because the amplitude of each entry of $\check{\mathbf{x}}_{\mathrm{ZF}}$ does matter in the decoding process. Because the fusion center does not have any knowledge of the squared norm of $\mathbf{x}$, the best way to normalize $\check{\mathbf{x}}_{\mathrm{ZF}}$ is

$$\|\check{\mathbf{x}}_{\mathrm{ZF}}\|^2 = N_t$$

assuming the elements of $\mathbf{x}$ are uniformly distributed from $\mathcal{S}$.

Finally, the fusion center needs to detect $\hat{\mathbf{x}}_{\mathrm{ZF}} = [\,\hat{x}_{\mathrm{ZF},1} \quad \hat{x}_{\mathrm{ZF},2} \quad \cdots \quad \hat{x}_{\mathrm{ZF},N_t}\,]^T$ by selecting the closest constellation point from $\check{\mathbf{x}}_{\mathrm{ZF}} = [\,\check{x}_{\mathrm{ZF},1} \quad \check{x}_{\mathrm{ZF},2} \quad \cdots \quad \check{x}_{\mathrm{ZF},N_t}\,]^T$ as

$$\hat{x}_{\mathrm{ZF},n} = \underset{s' \in \mathcal{S}}{\operatorname{argmin}} |\check{x}_{\mathrm{ZF},n} - s'|^2 \tag{14}$$

for $n = 1, \ldots, N_t$. The complexity of the ZF-type receiver is much lower than that of the ML receiver because each of these minimizations is over a set of $M$ elements.

### C. Receiver Performance

In this subsection, we analyze the performance of ML and ZF-type estimators where the entries of the estimates can be arbitrary complex numbers. We assume $\|\mathbf{x}\|^2 = N_t$ in this subsection. The following lemma shows the behavior of the ML estimator in the asymptotic regime of $K$ for arbitrary $\rho > 0$.

*Lemma 2:* Let $\check{\mathbf{x}}_{\mathrm{ML}}$ be the outcome of the ML estimator

$$\check{\mathbf{x}}_{\mathrm{ML}} = \underset{\substack{\mathbf{x}' \in \mathbb{C}^{N_t}, \\ \|\mathbf{x}'\|^2 = N_t}}{\operatorname{argmax}} L(\mathbf{x}').$$

For arbitrary $\rho > 0$, $\check{\mathbf{x}}_{\mathrm{ML}}$ converges to the true transmitted vector $\mathbf{x}$ in probability, i.e.,

$$\check{\mathbf{x}}_{\mathrm{ML}} \xrightarrow{p} \mathbf{x}$$

as $K \to \infty$.

*Proof:* We consider the real domain in the proof to simplify notation. The lemma can be proved by showing the inequality

$$L(\mathbf{x}_{\mathrm{R}}) > L(\mathbf{u}_{\mathrm{R}})$$

in probability for any $\mathbf{u}_{\mathrm{R}} \in \mathbb{R}^{2N_t} \setminus \{\mathbf{x}_{\mathrm{R}}\}$ with the constraint $\|\mathbf{u}_{\mathrm{R}}\|^2 = N_t$ when $K \to \infty$ for arbitrary $\rho > 0$. We take logarithm of the likelihood function and have

$$\begin{aligned}\log L(\mathbf{x}^{\ddagger}) &= \log\left(\prod_{i=1}^{2}\prod_{k=1}^{K} \Phi\left(\sqrt{\frac{2\rho}{N_t}}\widetilde{\mathbf{h}}_{\mathrm{R},k,i}^T \mathbf{x}^{\ddagger}\right)\right) \\ &= \sum_{i=1}^{2}\sum_{k=1}^{K} \log \Phi\left(\sqrt{\frac{2\rho}{N_t}}\widetilde{\mathbf{h}}_{\mathrm{R},k,i}^T \mathbf{x}^{\ddagger}\right).\end{aligned}$$

Because the $\widetilde{\mathbf{h}}_{\mathrm{R},k,i}$'s are independent for all $k$,

$$\lim_{K\to\infty} \frac{1}{K}\sum_{k=1}^{K} \log \Phi\left(\sqrt{\frac{2\rho}{N_t}}\widetilde{\mathbf{h}}_{\mathrm{R},k,i}^T \mathbf{x}^{\ddagger}\right) \xrightarrow{p} \mathrm{E}\left[\log \Phi\left(\sqrt{\frac{2\rho}{N_t}}\widetilde{\mathbf{h}}_{\mathrm{R},k,i}^T \mathbf{x}^{\ddagger}\right)\right]$$

by the weak law of large numbers, and we have

$$\frac{1}{K}\log L(\mathbf{x}^{\ddagger}) \xrightarrow{p} 2\mathrm{E}\left[\log \Phi\left(\sqrt{\frac{2\rho}{N_t}}\widetilde{\mathbf{h}}_{\mathrm{R},k,i}^T \mathbf{x}^{\ddagger}\right)\right]$$

as $K \to \infty$ where the expectation is taken over the channel.

Then, we need to show that

$$\mathrm{E}\left[\log \Phi\left(\sqrt{\frac{\rho}{N_t}}\widetilde{\mathbf{h}}_{\mathrm{R},k,i}^T \mathbf{x}_{\mathrm{R}}\right)\right] > \mathrm{E}\left[\log \Phi\left(\sqrt{\frac{\rho}{N_t}}\widetilde{\mathbf{h}}_{\mathrm{R},k,i}^T \mathbf{u}_{\mathrm{R}}\right)\right]$$

where the expectations are taken over the channel. Because $\log \Phi(\cdot)$ is a strictly monotonically increasing concave function, the above inequality is true if $\widetilde{\mathbf{h}}_{\mathrm{R},k,i}^T \mathbf{x}_{\mathrm{R}}$ first-order stochastically dominates $\widetilde{\mathbf{h}}_{\mathrm{R},k,i}^T \mathbf{u}_{\mathrm{R}}$ [34]. In Appendix B, we show

$$\widetilde{\mathbf{h}}_{\mathrm{R},k,i}^T \mathbf{x}_{\mathrm{R}} \overset{d}{>} \widetilde{\mathbf{h}}_{\mathrm{R},k,i}^T \mathbf{u}_{\mathrm{R}} \tag{15}$$

conditioned on the received signal $y_{\mathrm{R},k,i}$ where $\overset{d}{>}$ denotes strict first-order stochastic dominance. ■

We define the MSE between $\mathbf{x}$ and $\check{\mathbf{x}}$ as

$$\mathrm{MSE} = \frac{1}{N_t}\mathrm{E}\left[\|\mathbf{x} - \check{\mathbf{x}}\|^2\right]$$

where the expectation is taken over the realizations of channel and noise. The following corollary shows the MSE performance of the ML estimator in the asymptotic regime of $K$ for arbitrary $\rho > 0$.

*Corollary 1:* The MSE of the ML estimator converges to zero, i.e.,

$$\lim_{K\to\infty} \mathrm{MSE}_{\mathrm{ML}} \to 0$$

for arbitrary $\rho > 0$.

*Proof:* Note that the norm of $\mathbf{x}$ is bounded, i.e.,

$$\|\mathbf{x}\|^2 = N_t < \infty.$$

The convergence in probability of a random variable with a bounded norm implies the convergence in mean-square sense [35]. Thus, we have

$$\lim_{K\to\infty} \mathrm{E}\left[\|\mathbf{x} - \check{\mathbf{x}}_{\mathrm{ML}\|}\|^2\right]$$

which finishes the proof. ■

This analytical derivation for the ML estimator shows that the proposed ML receiver can perfectly decode the transmitted vector in the limit as $K$ grows large with fixed $\rho$. Moreover, numerical studies in Section IV show that increasing $\rho$ would be sufficient for the ML receiver to decode the transmitted vector correctly with fixed, but sufficiently large, $K$.

We now analyze the MSE of the ZF-type estimator. Although it is difficult to derive the MSE of the ZF-type estimator in general, we are able to have a closed-form expression for $\mathrm{MSE}_{\mathrm{ZF}}$ by approximating quantization loss as additional Gaussian noise where the approximation is frequently adopted in many frame expansion works, e.g., [31], [32], [36].

*Lemma 3:* If we approximate the quantization error using an additional Gaussian noise $\mathbf{w}$ as

$$\hat{\mathbf{y}} = \sqrt{\frac{\rho}{N_t}}\mathbf{H}\mathbf{x} + \mathbf{n} + \mathbf{w} \tag{16}$$

with[6] $\mathbf{w} \sim \mathcal{CN}(\mathbf{0}_K, \sigma_q^2 \frac{\rho}{N_t}\mathbf{I}_K)$ and assume $\mathbf{H}^H\mathbf{H} = K\mathbf{I}_{N_t}$, the MSE of the ZF-type estimator is given as[7]

$$\mathrm{MSE}_{\mathrm{ZF}} = \mathrm{E}\left[\left\|\mathbf{x} - \sqrt{N_t}\frac{\check{\mathbf{x}}_{\mathrm{ZF}}}{\|\check{\mathbf{x}}_{\mathrm{ZF}}\|}\right\|^2\right] = \frac{N_t\rho^{-1} + \sigma_q^2}{K}$$

where $\check{\mathbf{x}}_{\mathrm{ZF}}$ is defined in (13).

*Proof:* Because $\mathbf{n}$ and $\mathbf{w}$ are independent, (16) can be rewritten as

$$\hat{\mathbf{y}} = \sqrt{\frac{\rho}{N_t}}\mathbf{H}\mathbf{x} + \mathbf{n}'$$

with $\mathbf{n}' \sim \mathcal{CN}(\mathbf{0}_K, (1 + \sigma_q^2\frac{\rho}{N_t})\mathbf{I}_K)$. Applying Proposition 1 in [31] with appropriate normalization, $\mathrm{MSE}_{\mathrm{ZF}}$ can be bounded as

$$\frac{K\left(N_t\rho^{-1} + \sigma_q^2\right)}{B^2} \le \mathrm{MSE}_{\mathrm{ZF}} \le \frac{K\left(N_t\rho^{-1} + \sigma_q^2\right)}{A^2} \qquad (17)$$

where $A$ and $B$ are fixed constants that satisfy

$$A\mathbf{I}_{N_t} \le \mathbf{H}^H\mathbf{H} \le B\mathbf{I}_{N_t}.$$

The matrix inequality $A\mathbf{I}_{N_t} \le \mathbf{H}^H\mathbf{H}$ means that the matrix $\mathbf{H}^H\mathbf{H} - A\mathbf{I}_{N_t}$ is a positive semidefinite matrix. Due to the assumption on the channel matrix, we have

$$A = B = K,$$

and the lower and upper bounds in (17) both become $\frac{N_t\rho^{-1}+\sigma_q^2}{K}$, which finishes the proof. ∎

*Remark 3:* Note that the assumption $\mathbf{H}^H\mathbf{H} = K\mathbf{I}_{N_t}$ in Lemma 3 can be satisfied in the limit as the number of receive nodes grows large because

$$\mathbf{H}^H\mathbf{H} \xrightarrow{p} K\mathbf{I}_{N_t}$$

as $K \to \infty$ under our $\mathcal{CN}(0,1)$ i.i.d. channel assumption [37].

*Remark 4:* It is well known that the Gaussian approximation is the worst case additive noise and gives a lower bound on the mutual information [38]. Due to the inversely proportional (although implicit) relation between the mutual information and the MSE, we expect that the derivation in Lemma 3 would give an upper bound on the MSE of the ZF-type estimator. This is verified in Section IV with numerically obtained $\sigma_q^2$.

We also have the following corollary when $\rho$ becomes large.

*Corollary 2:* With the same assumptions used in Lemma 3, the MSE of the ZF-type estimator is given as

$$\mathrm{MSE}_{\mathrm{ZF}} = \frac{\sigma_q^2}{K}$$

when $\rho$ goes to infinity.

*Proof:* The proof of Corollary 2 is a direct consequence of taking the limit $\rho \to \infty$ on the result of Lemma 3. ∎

Lemma 3 and Corollary 2 show that we can make $\mathrm{MSE}_{\mathrm{ZF}}$ arbitrarily small by increasing $K$ regardless of the effect of noise or quantization error. However, due to the quantization process at each receive node, we have $\sigma_q^2 > 0$, and $\mathrm{MSE}_{\mathrm{ZF}}$ never goes to zero with fixed $K$ even when $\rho \to \infty$, which gives an error rate floor in the high SNR regime. These MSE analyses are based on the ZF-type estimator and the approximation of the quantization process in (16); however, the numerical results in Section IV show that the analyses also hold for the SER case with actual quantization process using the proposed ZF-type receiver.

[6]The constant $\frac{\rho}{N_t}$ in the variance of $\mathbf{w}$ is to reflect the effect of SNR in the quantization error.

[7]$\check{\mathbf{x}}_{\mathrm{ZF}}$ is normalized to have the same norm as $\mathbf{x}$.

### D. Modified Zero-Forcing-Type Receiver

As mentioned in the previous subsection, the ZF-type receiver suffers from an error rate floor when $\rho$ goes to infinity with fixed $K$. Although the error rate floor is indeed inevitable with the ZF-type receiver, we can improve the SER of the ZF-type receiver in the high SNR regime by performing post-processing for $\hat{\mathbf{x}}_{\mathrm{ZF}}$ given in (14).

When $\rho \to \infty$, the effect of noise disappears, and we have

$$\widetilde{\mathbf{H}}_{\mathrm{R,S}}\mathbf{x}_{\mathrm{R}} \succeq \mathbf{0}_{2K}$$

by the sign adjustment, where $\widetilde{\mathbf{H}}_{\mathrm{R,S}}$ is defined in (5), $\mathbf{x}_{\mathrm{R}}$ is the transmitted vector in the real domain, and $\succeq$ represents element-wise inequality. This fact also recalls the positive constraint on $t_\ell(\mathbf{x}'_{\mathrm{R}})$ in (7) used to upper bound the maximum of $L(\mathbf{x}'_{\mathrm{R}})$. Even in the high SNR regime, however, the $\hat{\mathbf{x}}_{\mathrm{ZF}}$ that is estimated from the ZF-type receiver may not satisfy the inequality constraints, which would cause an error rate floor. Thus, we formulate a linear program as

$$\max_{\hat{\mathbf{x}}_{\mathrm{R}} \in \mathbb{R}^{2N_t}} \quad \hat{\mathbf{x}}_{\mathrm{ZF}}^T\hat{\mathbf{x}}_{\mathrm{R}} \qquad \text{s.t.} \quad \widetilde{\mathbf{H}}_{\mathrm{R,S}}\hat{\mathbf{x}}_{\mathrm{R}} \succeq \mathbf{0}_{2K}$$

to force the estimate $\hat{\mathbf{x}}_{\mathrm{R}}$ to satisfy the inequality constraints. The estimate $\hat{\mathbf{x}}_{\mathrm{R}}$ should be mapped to $\mathcal{S}$ as in (14) before decoding.

It was shown in [31] that in the context of frame expansion without any noise, the reconstruction method by linear programming can give a MSE proportional to $\frac{1}{K^2}$, which is much better than the ZF-type receiver which results in a MSE proportional to $\frac{1}{K}$. However, if $\rho$ is not large enough, this post-processing by linear programming can cause performance degradation because the sign refinement may not be perfect, resulting in incorrect inequality constraints for the linear programming. Moreover, in this case, having more receive nodes may cause more errors due to the higher chance of having wrong inequality constraints. Note that more receive nodes corresponds to more rows in $\widetilde{\mathbf{H}}_{\mathrm{R,S}}$ that force more inequality constraints. We numerically evaluate the modified ZF-type receiver in Section IV.

### E. Achievable Rate Analysis

We can obtain the achievable rate of quantized distributed reception by evaluating the mutual information between the transmitted vector $\mathbf{x}$ and the quantized received signal $\hat{\mathbf{y}}$ given channel realization $\mathbf{H}$. If we assume $\mathbf{x}$ is uniformly distributed, i.e., $\Pr(\mathbf{x}) = \frac{1}{M^{N_t}}$, then the mutual information can be written as[8]

$$I(\mathbf{H}) = \frac{1}{M^{N_t}}\sum_{\mathbf{x}\in\mathcal{S}^{N_t}}\sum_{\hat{\mathbf{y}}\in\mathcal{Y}}\Pr(\hat{\mathbf{y}} \mid \mathbf{H}, \mathbf{x}) \times \log_2\left(\frac{\Pr\left(\hat{\mathbf{y}} \mid \mathbf{H}, \mathbf{x}\right)}{\frac{1}{M^{N_t}}\sum_{\mathbf{x}'\in\mathcal{S}^{N_t}}\Pr(\hat{\mathbf{y}} \mid \mathbf{H}, \mathbf{x}')}\right)$$

[8]Although the mutual information also depends on $\rho$ and $N_t$, we omit them for brevity.

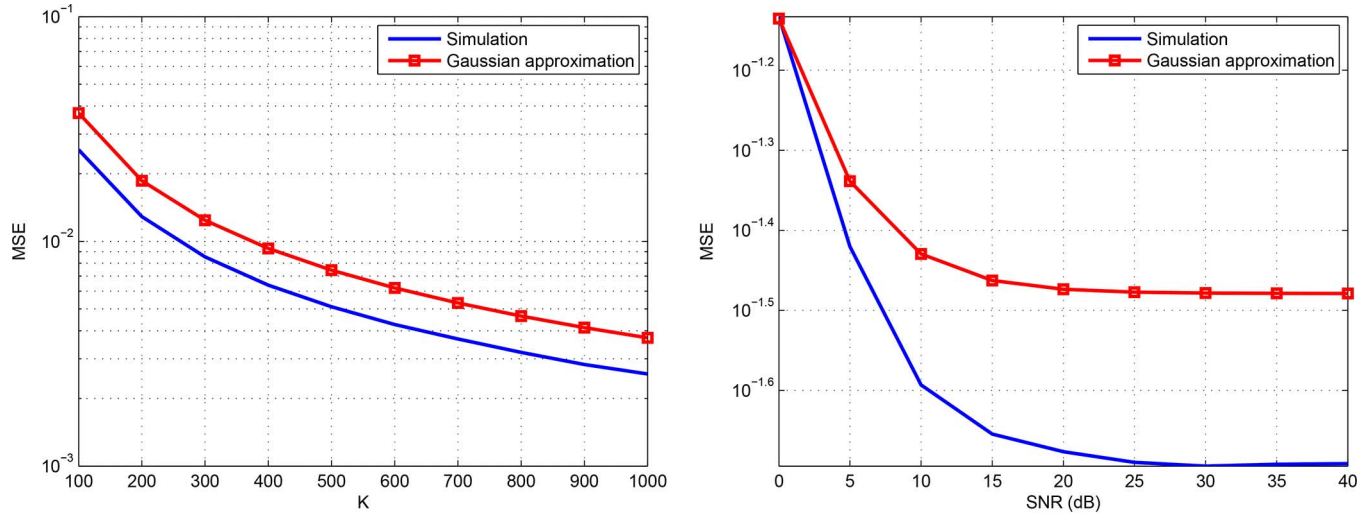


Fig. 2. The MSE of the ZF-type estimator and its approximation in Lemma 3 with increasing either of $K$ or $\rho$. We set $M = 8$ (8PSK) and $N_t = 4$ for both figures. (a) $\rho = 10$. (b) $K = 100$.

where $\mathcal{Y}$ is the set of all $(2^2)^K$ possible outcomes of the quantized received signal. Then, the average achievable rate is given as

$$R_{\text{ach}} = \mathrm{E}[I(\mathbf{H})] \tag{18}$$

where the expectation is taken over $\mathbf{H}$.

In general, it is difficult to obtain $I(\mathbf{H})$ analytically or numerically [39]. However, we are able to calculate $I(\mathbf{H})$ using the quantization structure in our problem. With the real domain notation in Section III.A, we have

$$\Pr\left(\hat{\mathbf{y}} \mid \mathbf{H}, \mathbf{x}\right) = \prod_{i=1}^{2}\prod_{k=1}^{K} \Pr\left(\hat{y}_{\mathrm{R},k,i} \mid \mathbf{h}_{\mathrm{R},k,i}, \mathbf{x}_{\mathrm{R}}\right).$$

Moreover, the probability of $\hat{y}_{\mathrm{R},k,i} = 1$ can be derived as

$$\begin{aligned}\Pr(\hat{y}_{\mathrm{R},k,i} = 1 \mid \mathbf{h}_{\mathrm{R},k,i}, \mathbf{x}_{\mathrm{R}}) &= \Pr\left(\sqrt{\frac{\rho}{N_t}}\mathbf{h}_{\mathrm{R},k,i}^T\mathbf{x}_{\mathrm{R}} \geq -n_{\mathrm{R},k,i}\right)\\ &= \Phi\left(\sqrt{\frac{2\rho}{N_t}}\mathbf{h}_{\mathrm{R},k,i}^T\mathbf{x}_{\mathrm{R}}\right).\end{aligned}$$

Similarly, we have

$$\Pr\left(\hat{y}_{\mathrm{R},k,i} = -1 \mid \mathbf{h}_{\mathrm{R},k,i}, \mathbf{x}_{\mathrm{R}}\right) = 1 - \Phi\left(\sqrt{\frac{2\rho}{N_t}}\mathbf{h}_{\mathrm{R},k,i}^T\mathbf{x}_{\mathrm{R}}\right).$$

Using these probabilities, we can calculate $I(\mathbf{H})$ numerically for given $\mathbf{H}$ and $\mathbf{x}$.

## IV. Numerical Results

In this section, we evaluate the proposed techniques with Monte Carlo simulations. We first evaluate the MSE of the ZF-type estimator and its analytical approximation derived in Lemma 3 where $\sigma_q^2$ in Lemma 3 is obtained numerically by averaging the empirical variance of the distribution[9] $(\mathbf{y} - \hat{\mathbf{y}})$ with different values of SNRs. The ML estimator is not considered in this simulation because it is computationally impractical to search over the (norm-constrained) $N_t$-dimensional complex space for the ML estimator. In Fig. 2(a), we increase $K$ with fixed $\rho = 10$ (i.e., an SNR of[10] 10 dB) while we increase $\rho$ with fixed $K = 100$ in Fig. 2(b). We set $N_t = 4$ and $M = 8$ (8PSK) in both figures. It is clear that the MSE of the ZF-type estimator is certainly bounded with fixed $K$ as $\rho$ becomes larger. However, if $K$ becomes larger, the MSE of the ZF-type estimator decreases without bound. As mentioned in Remark 4, the additive Gaussian noise approximation for the quantization error gives an upper bound for the MSE of the ZF-type estimator.

To see the diversity gain of each receiver, we consider the average SER which is defined as

$$\text{SER} = \frac{1}{N_t}\sum_{n=1}^{N_t} \mathrm{E}\left[\Pr\left(\hat{x}_n \neq x_n \mid \mathbf{x} \text{ sent}, \mathbf{H}, \mathbf{n}, \rho, N_t, K, \mathcal{S}\right)\right]$$

where the expectation is taken over $\mathbf{x}$, $\mathbf{H}$, and $\mathbf{n}$. We compare the SERs of ML and ZF-type (without the modification by the linear programming) receivers regarding the transmit SNR $\rho$ in dB scale with different values of $N_t$ and $M$ in Fig. 3. Note that both figures are for the case of 12 bits transmission per channel use because the total number of bits transmitted per channel use is given as

$$B_{\text{tot}} = N_t \log_2 M.$$

It is clear from the figures that as $\rho$ or $K$ increase, the SER of the ML receiver becomes smaller without any bound while that of the ZF-type receiver is certainly bounded in the high SNR regime. However, the SER of the ZF-type receiver can be improved by increasing $K$, which is the same as the MSE results. The results show that the ZF-type receiver would be

[9] $\hat{\mathbf{y}}$ is the actual quantized received signal, not the approximation in (16).

[10] Recall that $\rho$ is related to total transmit power, not per antenna transmit power, in our system setup.

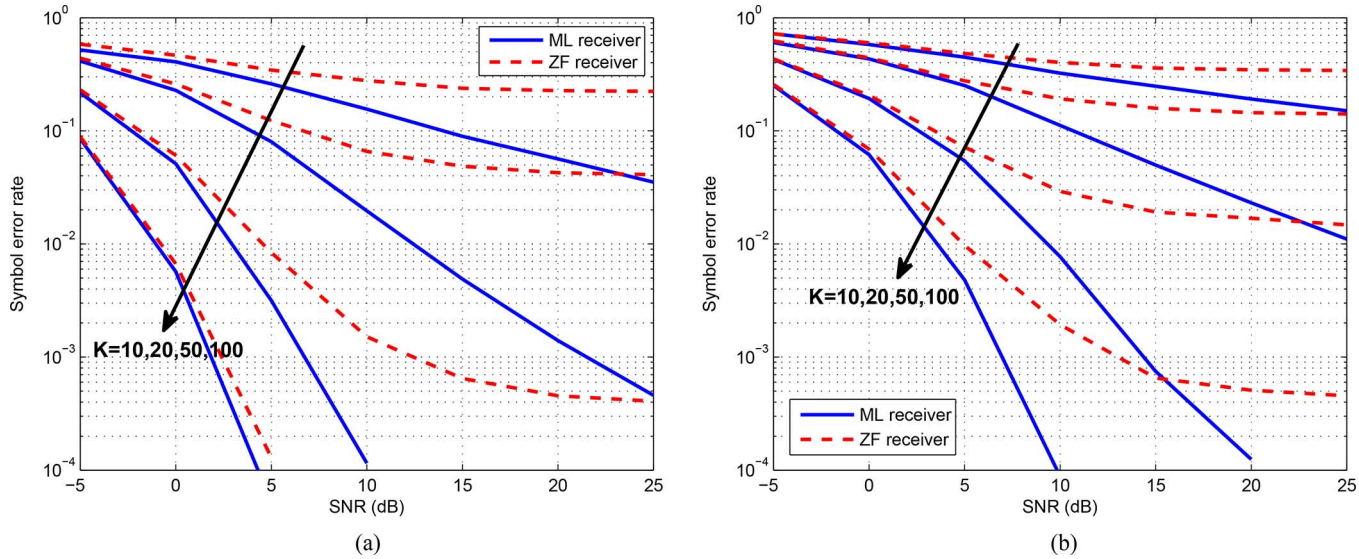


Fig. 3. SER vs. SNR in dB scale with different values of $N_t$ and $M$ for the constellation $\mathcal{S}$. Both figures are the case of 12 bits transmission per channel use. (a) $M = 4$ (QPSK) and $N_t = 6$. (b) $M = 8$ (8PSK) and $N_t = 4$.

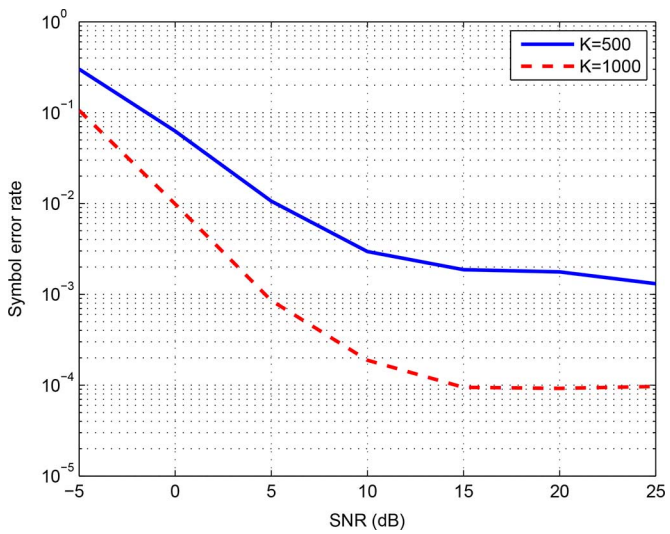


Fig. 4. SER vs. SNR in dB scale using the ZF-type receiver with $M = 16$ (16QAM) for the constellation $\mathcal{S}$ and $N_t = 10$.

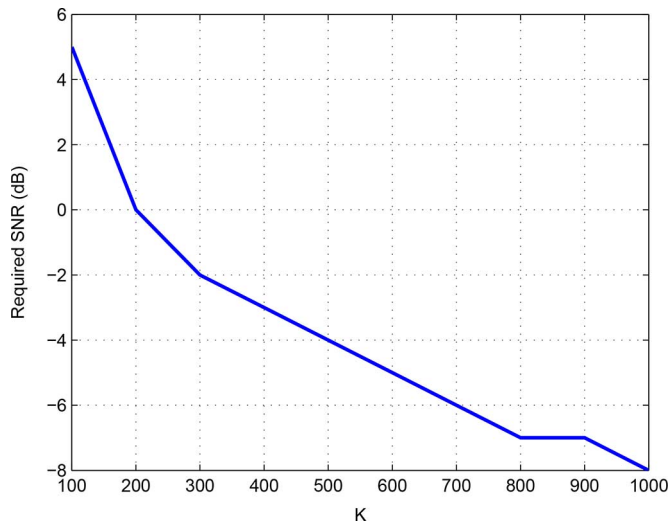


Fig. 5. Required SNR vs. $K$ for the ZF-type receiver to achieve the target SER of 0.01 with $N_t = 4$ and $M = 8$ (8PSK) for the constellation $\mathcal{S}$.

a good option for quantized distributed reception with a large number of receive nodes in the IoT environment.

Comparing these figures, if the number of transmit antennas $N_t$ at the transmitter is large, it is desirable to simultaneously transmit more symbols chosen from a smaller sized constellation to get better SER results when the number of transmitted bits per channel use, $B_{\text{tot}}$, is fixed for both the ML and ZF-type receivers. This result is suitable to massive MIMO systems where the transmitter is equipped with a large number of antennas.

We also plot the SERs of the ZF-type receiver[11] with a 16QAM constellation for $\mathcal{S}$ and $N_t = 10$ in Fig. 4. The figure shows that the proposed receiver also works for a non-PSK constellation even with not-so-large $N_t$. Thus, the norm constraint $\|\mathbf{x}\|^2 = N_t$ is not critical for the ZF-type receiver.

[11]We do not consider the ML receiver due to its excessive complexity.

To numerically evaluate the array gain, we plot the required SNR (in dB) for the ZF-type receiver to achieve the target SER of 0.01 against $K$ in Fig. 5. As the number of receive nodes increases, the required SNR to achieve the target SER decreases. Therefore, if we can exploit a large number of receive nodes, the transmitter may be able to rely on cost efficient power amplifiers with small transmit power.

In Fig. 6, we plot the SERs of the ZF-type receiver and a ZF-type receiver modified to use linear programming explained in Section III.D. We only consider the high SNR regime because the modified ZF-type receiver is aimed to increase the performance of the ZF-type receiver when the SNR is high. The figure clearly shows that the modified ZF-type receiver performs much better than the ZF-type receiver when the effect of noise becomes negligible; however, it performs worse than the ZF-type receiver when the SNR is not sufficiently high. Moreover, having more receive nodes deteriorates the performance of

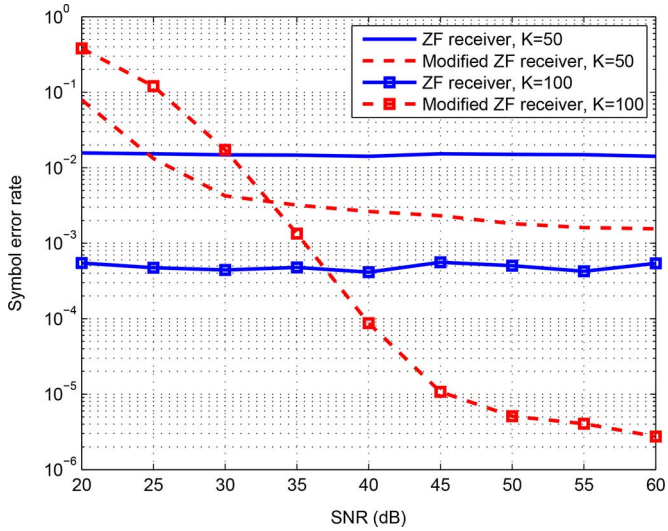


Fig. 6. SER vs. SNR in dB scale for the ZF-type and modified ZF-type receivers with $N_t = 4$ and $M = 8$ (8PSK) for the constellation $\mathcal{S}$.

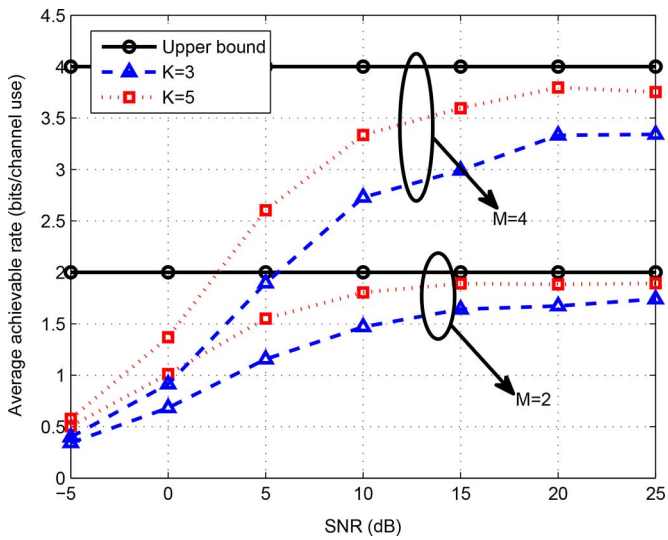


Fig. 7. Average achievable rates of quantized distributed reception vs. SNR with $N_t = 2$ and different values of $K$ and $M$.

the modified ZF-type receiver in this case, which is explained in Section III.D.

In Fig. 7, we plot the average achievable rate defined in (18) to evaluate the benefit of spatial multiplexing in distributed reception. Due to the computational complexity, we only consider $N_t = 2$ with $K = 3$ and 5 receive nodes.[12] Moreover, we limit the minimum value of $\Pr(\hat{y}_{\mathrm{R},k,i} \mid \mathbf{h}_{\mathrm{R},k,i}, \mathbf{x}_{\mathrm{R}})$ to 0.0001 to avoid numerical errors on $I(\mathbf{H})$. The figure shows that the achievable rates of quantized distributed reception for both $M = 2$ (BPSK) and 4 (QPSK) cases become close to its maximum value as $\rho$ increases even with small numbers of $K$. It is expected that we can achieve the maximum achievable rate with a not-so-large number of receive nodes, e.g., $K = 10$, with moderate SNR values.

[12]Because the size of $\mathcal{Y}$ is $(2^2)^K$, it quickly becomes computationally impractical as $K$ increases.

## V. Conclusion

In this paper, we studied a quantized distributed reception scenario where the transmitter is equipped with multiple transmit antennas and broadcasts multiple independent data symbols by spatial multiplexing to a set of geographically separated receive nodes through fading channels. Each receive node then processes its received signal and forwards it to the fusion center, and the fusion center tries to decode the transmitted data symbols by exploiting the forwarded information and global channel knowledge. We implemented an optimal ML receiver and a low-complexity ZF-type receiver for this scenario. The SER of the ML receiver can be made arbitrarily small by increasing SNR and the number of receive nodes. The ZF-type receiver suffers from an error rate floor as the SNR increases. This floor can be lowered by increasing the number of receive nodes.

The scenario studied in this paper, i.e., high data rate transmission by spatial multiplexing in quantized distributed reception, may become popular in the near future with the emergence of the Internet of Things (IoT) where we can easily have a numerous number of receive nodes. To make the scenario more practical, the fusion center may decode the transmitted symbols without global channel knowledge, which is an interesting future research topic.

## Appendix A

*Lemma:* For arbitrary $s$ and $c$ that satisfy $s > c > 0$, we have

$$(\Phi(s))^2 > \Phi(s+c)\Phi(s-c).$$

*Proof:* With $s > c > 0$, we have the inequality

$$\Phi(s) - \Phi(s-c) > \Phi(s+c) - \Phi(s).$$

Then, we have

$$2\Phi(s) > \Phi(s+c) + \Phi(s-c)$$

which is equivalent to

$$\begin{aligned} 4(\Phi(s))^2 &> (\Phi(s+c) + \Phi(s-c))^2 \\ &= (\Phi(s+c))^2 + (\Phi(s-c))^2 + 2\Phi(s+c)\Phi(s-c) \\ &\overset{(a)}{\geq} 4\Phi(s+c)\Phi(s-c) \end{aligned}$$

where $(a)$ is because

$$(\Phi(s+c) - \Phi(s-c))^2 \geq 0,$$

which finishes the proof. ■

## Appendix B
## Proof of First-Order Stochastic Dominance

We drop unnecessary subscripts to simplify notation. Recall that

$$y = \sqrt{\frac{\rho}{N_t}}\mathbf{h}^T\mathbf{x} + n,$$
$$\widetilde{\mathbf{h}} = \hat{y}\mathbf{h}$$

where $\hat{y} = \text{sgn}(y)$. Using the fact that $\mathbf{h}$ is rotationally invariant, we assume the transmitted vector is given as[13] $\mathbf{x} = [\sqrt{N_t} \quad 0 \quad \cdots \quad 0]^T$. Then, we have

$$y = \sqrt{\rho} h_1 + n.$$

Because $y \sim \mathcal{N}(0, \frac{\rho+1}{2})$ and $n \sim \mathcal{N}(0, \frac{1}{2})$, the distribution of $\sqrt{\rho} h_1$ conditioned on $y$ is $\mathcal{N}(\mu, \gamma^2)$ where

$$\mu = \frac{\rho}{\rho+1} y, \quad \gamma^2 = \frac{\rho}{2(\rho+1)}.$$

Let $c = \frac{\rho}{\rho+1}$. Then, we can write $\sqrt{\rho} h_1 = cy + w$ where $w \sim \mathcal{N}(0, \gamma^2)$. Moreover, we have

$$\sqrt{\frac{\rho}{N_t}} \widetilde{\mathbf{h}}^T \mathbf{x} = \sqrt{\rho} \hat{y} h_1 = c|y| + \hat{y} w \stackrel{d}{=} |cy| + w$$

conditioned on $y$ where the third equality comes from the independence of $\hat{y}$ and $w$. Note that $\stackrel{d}{=}$ denotes stochastic equivalence.

Now we want to compute the distribution of $\sqrt{\frac{\rho}{N_t}} \widetilde{\mathbf{h}}^T \mathbf{u}$ for a fixed $\mathbf{u}$ given $y$. Note that

$$\mathbf{h}^T \mathbf{u} = \sum_{i=1}^{2N_t} h_i u_i \stackrel{d}{=} u_1 h_1 + z\sqrt{N_t - u_1^2}$$

where $z \sim \mathcal{N}(0, \frac{1}{2})$. Then, we have

$$\begin{aligned}
\sqrt{\frac{\rho}{N_t}} \widetilde{\mathbf{h}}^T \mathbf{u} &\stackrel{d}{=} \frac{u_1}{\sqrt{N_t}}(c|y| + w) + \hat{y} z \sqrt{\rho\left(1 - \frac{u_1^2}{N_t}\right)} \\
&\stackrel{d}{=} \frac{u_1}{\sqrt{N_t}}(c|y| + w) + z \sqrt{\rho\left(1 - \frac{u_1^2}{N_t}\right)} \\
&= u(c|y| + w) + z\sqrt{\rho(1-u^2)}
\end{aligned}$$

where the second equality is due to the independence of $\hat{y}$ and $z$ and the third equality comes from the variable substitution $u = \frac{u_1}{\sqrt{N_t}}$. Note that $-1 \le u < 1$. If $u = 1$, then $\mathbf{u}$ becomes $\mathbf{x}$, which violates our assumption.

We now break up $uw + z\sqrt{\rho(1-u^2)}$ into two independent zero-mean Gaussian random variables $v_1$ and $v_2$ where

$$v_1 \sim \mathcal{N}\left(0, (1-u^2)\frac{\rho^2}{2(\rho+1)}\right), \quad v_2 \sim \mathcal{N}(0, \gamma^2).$$

Finally, for a given $y$, we have

$$\begin{aligned}
\sqrt{\frac{\rho}{N_t}} \widetilde{\mathbf{h}}^T \mathbf{u} &\stackrel{d}{=} u(c|y| + w) + z\sqrt{\rho(1-u^2)} \\
&= uc|y| + v_1 + v_2 \\
&\stackrel{d}{<} |uc|y| + v_1| + v_2 \qquad (19) \\
&= |ucy + \hat{y} v_1| + v_2 \\
&\stackrel{d}{=} |ucy + v_1| + v_2 \qquad (20) \\
&\stackrel{d}{=} |cy| + w \qquad (21) \\
&\stackrel{d}{=} \sqrt{\frac{\rho}{N_t}} \widetilde{\mathbf{h}}^T \mathbf{x}.
\end{aligned}$$

[13]In this proof, we do not have to restrict the elements of $\mathbf{x}$ from an $M$-ary constellation $\mathcal{S}$ because we consider the ML estimator not receiver.

To show the strict stochastic dominance in (19), recall that $uc|y|$ is a fixed number given $y$, and $v_1$ is a Gaussian random variable. Thus, the complementary cumulative distribution function of $|uc|y| + v_1|$ should be strictly greater than that of $uc|y| + v_1$. The stochastic equivalence in (20) is because $\hat{y}$ and $v_1$ are independent and (21) is due to the facts that

$$ucy + v_1 \sim \mathcal{N}\left(0, \frac{\rho^2}{2(\rho+1)}\right), \quad cy \sim \mathcal{N}\left(0, \frac{\rho^2}{2(\rho+1)}\right)$$

and $v_2 \stackrel{d}{=} w$. Thus, (15) holds, and we have the claim.

## REFERENCES


[1] L. Atzori, A. Iera, and G. Morabito, "The internet of things: A survey," *Elsevier Comput. Netw.*, vol. 54, no. 15, pp. 2787–2805, Oct. 2010.

[2] R. S. Blum, "Distributed detection for diversity reception of fading signals in noise," *IEEE Trans. Inf. Theory*, vol. 45, no. 1, pp. 158–164, Jan. 1999.

[3] R. Irmer, H. Droste, P. Marsch, M. Grieger, G. Fettweis, S. Brueck, H.-P. Mayer, L. Thiele, and V. Jungnickel, "Coordinated multipoint: Concepts, performance, and field trial results," *IEEE Commun. Mag.*, vol. 49, no. 2, pp. 102–111, Feb. 2011.

[4] *Coordinated Multi-Point Operation for LTE Physical Layer Aspects (Release 11)*, 3GPP TR 36.819 Std., 2011.

[5] *Coordinated Multi-Point in Mobile Communications: From Theory to Practice*, P. Marsch and G. P. Fettweis, Eds. Cambridge, UK: Cambridge Univ. Press, 2011.

[6] D. Lee, H. Seo, B. Clerckx, E. Hardouin, D. Mazzarese, S. Nagata, and K. Sayana, "Coordinated multipoint transmission and reception in LTE-Advanced: Deployment scenarios and operational challenges," *IEEE Commun. Mag.*, vol. 50, no. 2, pp. 148–155, Feb. 2012.

[7] S. Park, O. Simeone, O. Sahin, and S. Shamai, "Joint precoding and multivariate backhaul compression for the downlink of cloud radio access networks," *IEEE Trans. Signal Process.*, vol. 61, no. 22, pp. 5646–5658, Nov. 2013.

[8] J. Kang, O. Simeone, J. Kang, and S. Shamai, "Joint signal and channel state information compression for the backhaul of uplink network MIMO systems," *IEEE Trans. Wireless Commun.*, vol. 13, no. 3, pp. 1555–1567, Mar. 2014.

[9] S. Park, O. Simeone, O. Sahin, and S. Shamai, "Fronthaul compression for cloud radio access networks: Signal processing advances inspired by network information theory," *IEEE Signal Process. Mag.*, vol. 31, no. 6, pp. 69–79, Nov. 2014.

[10] I. F. Akyildiz, W. Su, Y. Sankarasubramaniam, and E. Cayirci, "A survey on sensor networks," *IEEE Commun. Mag.*, vol. 40, no. 8, pp. 102–114, Aug. 2002.

[11] V. Mhatre and C. Rosenberg, "Design guidelines for wireless sensor networks: Communication, clustering and aggregation," *Ad Hoc Netw.*, vol. 2, no. 1, pp. 45–63, Jan. 2004.

[12] J. Yick, B. Mukherjee, and D. Ghosal, "Wireless sensor network survey," *Comput. Netw.*, vol. 52, no. 12, pp. 2292–2330, Aug. 2008.

[13] P. Varshney, *Distributed Detection and Data Fusion*. New York, NY, USA: Springer, 1997.

[14] A. Nayagam, J. Shea, and T. Wong, "Collaborative decoding in bandwidth-constrained environments," *IEEE J. Sel. Areas Commun.*, vol. 25, no. 2, pp. 434–446, Feb. 2007.

[15] A. Sanderovich, S. Shamai, Y. Steinberg, and G. Kramer, "Communication via decentralized processing," *IEEE Trans. Inf. Theory*, vol. 54, no. 7, pp. 3008–3023, Jul. 2008.

[16] R. Viswanathan and P. K. Varshney, "Distributed detection with multiple sensors: Part I—fundamentals," *Proc. IEEE*, vol. 85, no. 1, pp. 54–63, Jan. 1997.

[17] A. Ribeiro and G. B. Giannakis, "Bandwidth-constrained distributed estimation for wireless sensor networks—Part I: Gaussian case," *IEEE Trans. Signal Process.*, vol. 54, no. 3, pp. 1131–1143, Mar. 2006.

[18] A. Ribeiro and G. B. Giannakis, "Bandwidth-constrained distributed estimation for wireless sensor networks—Part II: Unknown probability density function," *IEEE Trans. Signal Process.*, vol. 54, no. 7, pp. 2784–2796, Jul. 2006.

[19] T.-Y. Wang, Y. S. Han, P. K. Varshney, and P.-N. Chen, "Distributed fault-tolerant classification in wireless sensor networks," *IEEE J. Sel. Areas Commun.*, vol. 23, no. 4, pp. 724–734, Apr. 2005.

[20] T.-Y. Wang, Y. S. Han, B. Chen, and P. K. Varshney, "A combined decision fusion and channel coding scheme for distributed fault-tolerant classification in wireless sensor networks," *IEEE Trans. Wireless Commun.*, vol. 5, no. 7, pp. 1695–1705, Jul. 2006.
[21] C. Yao, P.-N. Chen, T.-Y. Wang, Y. S. Han, and P. K. Varshney, "Performance analysis and code design for minimum Hamming distance fusion in wireless sensor networks," *IEEE Trans. Inf. Theory*, vol. 53, no. 5, pp. 1716–1734, May 2007.
[22] D. J. Love, J. Choi, and P. Bidigare, "Receive spatial coding for distributed diversity," in *Proc. IEEE Asilomar Conf. Signals, Syst., Comput.*, Nov. 2013.
[23] J. Choi, D. J. Love, and P. Bidigare, "Coded distributed diversity: A novel distributed reception technique for wireless communication systems," *IEEE Trans. Signal Process.* vol. 63, no. 5, pp. 1310–1321, Mar. 1, 2015.
[24] D. R. Brown, III, U. Madhow, M. Ni, M. Rebholz, and P. Bidigare, "Distributed reception with hard decision exchanges," *IEEE Trans. Wireless Commun.*, vol. 13, no. 6, pp. 3406–3418, Jun. 2014.
[25] J. Fang and H. Li, "Hyperplane-based vector quantization for distributed estimation in wireless sensor networks," *IEEE Trans. Inf. Theory*, vol. 55, no. 12, pp. 5682–5699, Dec. 2009.
[26] J. Fang and H. Li, "Optimal/near-optimal dimensionality reduction for distributed estimation in homogeneous and certain inhomogeneous scenarios," *IEEE Trans. Signal Process.*, vol. 58, no. 8, pp. 4339–4353, Aug. 2010.
[27] F. Rusek, D. Persson, B. K. Lau, E. G. Larsson, T. L. Marzetta, E. O. , and F. Tufvesson, "Scaling up MIMO: Opportunities and challenges with very large arrays," *IEEE Signal Process. Mag.*, vol. 30, no. 1, pp. 40–60, Jan. 2013.
[28] R. R. Tenney and N. R. Sandell, Jr., "Detection with distributed sensors," *IEEE Trans. Aerosp. Electron. Syst.*, vol. AES-17, no. 4, pp. 501–510, Jul. 1981.
[29] K. Vardhan, S. K. Mohammed, A. Chockalingam, and B. S. Rajan, "A low-complexity detector for large MIMO systems and multicarrier CDMA systems," *IEEE J. Sel. Areas Commun.*, vol. 26, no. 3, pp. 473–485, Apr. 2008.
[30] J. Choi, B. Lee, B. Shim, and I. Kang, "Low complexity soft-input soft-output group detection for massive MIMO systems," in *Proc. IEEE Int. Conf. Commun.*, Jun. 2013.
[31] V. K. Goyal, M. Vetterli, and N. T. Thao, "Quantized overcomplete expansions in $\mathbb{R}^n$: Analysis, synthesis, and algorithms," *IEEE Trans. Inf. Theory*, vol. 44, no. 1, pp. 16–30, Jan. 1998.
[32] V. K. Goyal and J. Kovac˘evi´c, "Quantized frame expansions with erasures," *Appl. Computat. Harmon. Anal.*, vol. 10, no. 3, pp. 203–233, May 2001.
[33] J. Choi, D. J. Love, and D. R. Brown, III, "Channel estimation techniques for quantized distributed reception in MIMO systems," in *Proc. IEEE Asilomar Conf. Signals, Syst., Comput.*, Nov. 2014.
[34] E. Wolfstetter, *Topics in Microeconomics: Industrial Organization, Auctions, and Incentives*. Cambridge, UK: Cambridge Univ. Press, 1999.
[35] A. Papoulis and S. U. Pillai, *Probability, Random Variables and Stochastic Processes*, 4th ed. New York, NY, USA: McGraw-Hill, 2002.
[36] J. J. Benedetto, A. M. Powell, and Ö. Yılmaz, "Sigma-delta $(\Sigma\Delta)$ quantization and finite frames," *IEEE Trans. Signal Process.*, vol. 52, no. 5, pp. 1990–2005, May 2006.
[37] T. L. Marzetta, "Noncooperative cellular wireless with unlimited numbers of base station antennas," *IEEE Trans. Wireless Commun.*, vol. 9, no. 11, pp. 3590–3600, Nov. 2010.
[38] B. Hassibi and B. M. Hochwald, "How much training is needed in multiple-antenna wireless links?," *IEEE Trans. Inf. Theory*, vol. 49, no. 4, pp. 951–963, Apr. 2003.
[39] B. M. Hochwald and S. Ten Brink, "Achieving near-capacity on a multiple-antenna channel," *IEEE Trans. Commun.*, vol. 51, no. 3, pp. 389–399, Mar. 2008.

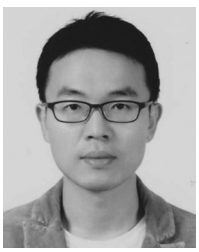

**Junil Choi** (S'12–M'15) received the B.S. (with honors) and M.S. degrees in electrical engineering from Seoul National University, Korea, in 2005 and 2007, respectively, and received the Ph.D. degree in electrical and computer engineering from Purdue University, West Lafayette, IN, USA, in 2015.

He is now a Postdoctoral Fellow at The University of Texas at Austin, USA. From 2007 to 2011, he was a member of the Technical Staff at Samsung Electronics, Korea, where he contributed advanced codebook and feedback framework designs to 3GPP LTE-Advanced and IEEE 802.16m standards. His research interests are in the design and analysis of massive MIMO and distributed communication systems.

Dr. Choi was a corecipient of the 2013 IEEE Globecom Best Paper Award and the 2008 Global Samsung Technical Conference Best Paper Award. He was a recipient of the Michael and Katherine Birck Fellowship from Purdue University in 2011; the Korean Government Scholarship Program for Study Overseas in 2011–2013; the Purdue University ECE Graduate Student Association Outstanding Graduate Student Award in 2013; and the Purdue College of Engineering Outstanding Student Research Award in 2014. He was recognized as an Exemplary Reviewer of the IEEE WIRELESS COMMUNICATIONS LETTERS in 2013.

**David J. Love** (S'98–M'05–SM'09–F'15) received the B.S. (with highest honors), M.S.E., and Ph.D. degrees in electrical engineering from the University of Texas at Austin, USA, in 2000, 2002, and 2004, respectively.

During summer 2000 and 2002, he was with Texas Instruments, Dallas, USA. Since August 2004, he has been with the School of Electrical and Computer Engineering, Purdue University, West Lafayette, IN, USA, where he is now a Professor and recognized as a University Faculty Scholar. His research interests are in the design and analysis of communication systems, MIMO, massive MIMO, millimeter wave, and MIMO array processing. He has approximately 30 U.S. patent filings, 23 of which have issued.

Dr. Love has served as an Editor for the IEEE TRANSACTIONS ON COMMUNICATIONS, an Associate Editor for the IEEE TRANSACTIONS ON SIGNAL PROCESSING, and a Guest Editor for special issues of the IEEE JOURNAL ON SELECTED AREAS IN COMMUNICATIONS and the EURASIP *Journal on Wireless Communications and Networking*. He is a Fellow of the Royal Statistical Society, and he has been inducted into Tau Beta Pi and Eta Kappa Nu. He is recognized as a Thomson Reuters Highly Cited Researcher. He has received multiple paper awards including the 2009 IEEE Jack Neubauer Memorial Award for the best systems paper published in the IEEE TRANSACTIONS ON VEHICULAR TECHNOLOGY in that year.

**D. Richard Brown, III** (S'97–M'00–SM'09) received the B.S. and M.S. degrees in electrical engineering from The University of Connecticut, Storrs, USA, in 1992 and 1996, respectively, and received the Ph.D. degree in electrical engineering from Cornell University, Ithaca, NY, USA, in 2000.

From 1992 to 1997, he was with General Electric Electrical Distribution and Control. Since August 2000, he has been with the Department of Electrical and Computer Engineering, Worcester Polytechnic Institute (WPI), Worcester, MA, where he is now a Professor. He also held an appointment as a Visiting Associate Professor at Princeton University, Princeton, NJ, USA, from August 2007 to June 2008. His research interests are currently in coordinated wireless transmission and reception, synchronization, distributed computing, and game-theoretic analysis of communication networks.

**Mireille Boutin** was born in the province of Quebec in Canada. She received the B.Sc. degree in physics-mathematics from the University de Montreal, and the Ph.D. degree in mathematics from the University of Minnesota in Minneapolis under the direction of Peter Olver.

After postdoctoral study at Brown University followed by a postdoctoral position at the Max Planck Institute for Mathematics in the Sciences, Leipzig, Germany, she joined the School of Electrical and Computer Engineering, Purdue University, West Lafayette, IN, USA. She is now an Associate Professor with tenure, and holds a courtesy appointment in the Department of Mathematics. Her current research interests include "big data" problems such as object recognition and various applied mathematics problems including problems related to diet management and nutrition analysis.